Quantitative description of the ^{20}Ne(p, $p\alpha$)^{16}O reaction as a means of probing the surface α amplitude

Kazuki Yoshida,[1,2,*] Yohei Chiba,[3,4,2] Masaaki Kimura,[5,6,2] Yasutaka Taniguchi,[7,2]
Yoshiko Kanada-En'yo,[8,2] and Kazuyuki Ogata[2,3,4]

[1]*Advanced Science Research Center, Japan Atomic Energy Agency, Tokai, Ibaraki 319-1195, Japan*
[2]*Research Center for Nuclear Physics (RCNP), Osaka University, Ibaraki 567-0047, Japan*
[3]*Department of Physics, Osaka City University, Osaka 558-8585, Japan*
[4]*Nambu Yoichiro Institute of Theoretical and Experimental Physics (NITEP), Osaka City University, Osaka 558-8585, Japan*
[5]*Department of Physics, Hokkaido University, Sapporo 060-0810, Japan*
[6]*Nuclear Reaction Data Centre, Hokkaido University, Sapporo 060-0810, Japan*
[7]*Department of Information Engineering, National Institute of Technology (KOSEN), Kagawa College, Mitoyo, Kagawa 769-1192, Japan*
[8]*Department of Physics, Kyoto University, Kyoto 606-8502, Japan*

(Received 16 May 2019; published 3 October 2019)

Background: The proton-induced α knockout reaction has been utilized for decades to investigate the α cluster formation in the ground state of nucleus. However, even today, the theoretical description of the reaction is not precise enough for the quantitative study. For example, the α spectroscopic factors reduced from α knockout experiments with reaction analyses using phenomenological α cluster wave functions disagree with those given by a structure theory. In some cases they also scatter depending on the kinematical condition of the experiment. This suggests that the theoretical description of the α knockout reaction is insufficient from a quantitative viewpoint.

Purpose: We show that the distorted wave impulse approximation can describe ^{20}Ne(p, $p\alpha$)^{16}O reaction quantitatively if reliable inputs are used; the optical potential, the p-α cross section, and the α cluster wave function. We also investigate the relationship between the α cluster wave function and the α knockout cross section.

Method: The ^{20}Ne(p, $p\alpha$)^{16}O reaction is described by the distorted wave impulse approximation. An input of the calculation, the α-^{16}O cluster wave function, is obtained by the antisymmetrized molecular dynamics and the Laplace expansion method.

Results: In contrast to the previous work, the ^{20}Ne(p, $p\alpha$)^{16}O data at 101.5 MeV is successfully reproduced by the present framework without any free adjustable parameters. It is also found that the knockout cross section is sensitive to the surface region of the cluster wave function because of the peripherality of the reaction.

Conclusions: Using a reliable α cluster wave function, p-α cross section, and distorting potentials, it is found that the ^{20}Ne(p, $p\alpha$)^{16}O cross section is quantitatively reproduced by the present framework. This success demonstrates that the proton-induced α knockout reaction is a quantitative probe for the α clustering.

DOI: 10.1103/PhysRevC.100.044601

I. INTRODUCTION

As it is schematically illustrated in the Ikeda diagram [1], the α particle is expected to emerge as a subunit in nuclear systems, in the light mass region in particular, reflecting the fact that the α particle is a tightly bound system of four nucleons with the large first excitation energy compared to neighboring nuclei. Various cluster models have been developed so far, and in recent decades microscopic cluster models based on the nucleon degrees of freedom with fermionic quantum statistics are available, as reviewed in a recently published article [2]. Among them, the antisymmetrized molecular dynamics (AMD) has been applied to many systems and succeeded in describing cluster structures [3–12]. One of the questions remaining today is to what extent α cluster state exists in the nuclear ground states that lie far below the α threshold.

From a nuclear reaction point of view, the proton-induced α knockout reaction, (p, $p\alpha$), is considered to be a good probe for the α cluster state in the ground state of a target nucleus. Much effort has been made on the (p, $p\alpha$) reaction studies [13–23], but even today quantitative understanding of the (p, $p\alpha$) cross section and its relation with the α cluster wave function in the ground state of the target nucleus have not yet fully established. For example, in Ref. [15] it is reported that the α spectroscopic factor (S_α) of the α-^{16}O cluster state in the ground state of ^{20}Ne deduced from the ^{20}Ne(p, $p\alpha$)^{16}O experiment is 2.4–3.0 times as large as those given by structure theories. It is also reported in Ref. [20] that S_α of ^{12}C from the ^{12}C(p, $p\alpha$)^{8}Be reaction at 100 MeV

*yoshida.kazuki@jaea.go.jp

has large uncertainty of $S_\alpha = 0.19$–1.68 depending on the kinematics of the experiment, while S_α should be determined purely from the structure of ^{12}C and should not depend on the kinematical condition of the reaction. Those uncertainties may arise from the ambiguities in the reaction analyses, namely, the optical potentials, the α cluster wave function, and the p-α differential cross section and its energy and angular dependence.

Considering the above-mentioned situation, a qualitative description of the $(p, p\alpha)$ reaction is still challenging. In the present study, we aim to reproduce the ^{20}Ne$(p, p\alpha)^{16}$O cross section data [15] within the distorted wave impulse approximation (DWIA) framework [24,25]. Since the target and the residue of this reaction are typical stable nuclei and the distorting potentials of them are well known, the description of the reaction will be free from ambiguities of the optical potential. In addition, in the experiment the emission angles of the p and α are fixed and the corresponding p-α binary scattering angle is very limited. This may also help to reduce the ambiguity arising from the angular dependence of the p-α cross section required in the DWIA calculation. As for the α cluster wave function, the $\alpha + ^{16}$O reduced width amplitude (RWA) of the ^{20}Ne ground state obtained by the AMD framework [12] is adopted as an input of the DWIA calculation.

In Sec. II, the theoretical description of AMD and DWIA for the $\alpha + ^{16}$O cluster state and the ^{20}Ne$(p, p\alpha)^{16}$O reaction, respectively, are introduced. In Sec. III, numerical input for the calculations is explained, and a comparison between the obtained ^{20}Ne$(p, p\alpha)^{16}$O cross section and the experimental data are shown. The probed region of the reaction is also investigated by applying several Brink-Bloch wave functions [26] of the α-^{16}O cluster state to the reaction calculation. Finally, a summary is given in Sec. IV.

II. THEORETICAL FRAMEWORK

A. Reduced width amplitude

The RWA is the probability amplitude to find the clusters at intercluster distance R, and is defined as the overlap between the ground state wave function of ^{20}Ne and the reference wave function for the $\alpha + ^{16}$O clustering,

$$y(R) = \sqrt{\frac{20!}{16!4!4\pi}} \left\langle \frac{\delta(r-R)}{r^2} \Phi_\alpha \Phi_{^{16}\mathrm{O}} \middle| \Psi_{^{20}\mathrm{Ne}} \right\rangle. \quad (1)$$

The integral of the RWA called α spectroscopic factor S_α is often used as a measure of the clustering,

$$S_\alpha = \int_0^\infty R^2 dR |y(R)|^2. \quad (2)$$

In the definition of the RWA given by Eq. (1), the bra vector represents the reference cluster state, in which the α and ^{16}O clusters are coupled to angular momentum zero with the intercluster distance R. The ground state wave functions of the α and ^{16}O clusters (Φ_α and $\Phi_{^{16}\mathrm{O}}$) are the harmonic oscillator wave functions of double closed shell configurations. The ket state $\Psi_{^{20}\mathrm{Ne}}$ is the ground state wave function of ^{20}Ne calculated by AMD. The AMD wave function is a superposition of parity and angular momentum projected Slater determinants, and it was shown that the known properties of the ^{20}Ne ground and excited states such as the radius, energies, electromagnetic transitions, and α decay widths are reasonably described. Once the ground state wave function is obtained, Eq. (1) is calculated by using the Laplace expansion method [12]. For more details of the calculation, readers are directed to Refs. [6,9]. It should be noted that other cluster models yield similar RWA and reasonably reproduce the observed decay widths of the excited states [6,27–30]. The use of AMD in the present study is aimed to extend our framework to the investigation of the α clustering in unstable nuclei in the future.

B. Distorted wave impulse approximation

We employ the DWIA framework in the present study. Details of DWIA for the description of the knockout reaction can be found in a recent review paper [25]. The incident and emitted protons are labeled as particles 0 and 1, respectively. The wave number and its solid angle, the total and kinetic energies of particle i (=0, 1, α) are represented by $\boldsymbol{K}_i$, Ω_i, E_i, and T_i, respectively. Quantities with (without) the superscript L are evaluated in the laboratory (center-of-mass) frame.

The triple differential cross section (TDX) of the $A(p, p\alpha)B$ reaction within the so-called factorized form of the DWIA framework is given by

$$\frac{d^3\sigma}{dE_1^{\mathrm{L}} d\Omega_1^{\mathrm{L}} d\Omega_2^{\mathrm{L}}} = F_{\mathrm{kin}} C_0 \frac{d\sigma_{p\alpha}}{d\Omega_{p\alpha}}(\theta_{p\alpha}, T_{p\alpha}) \left|\bar{T}_{\boldsymbol{K}_i}\right|^2. \quad (3)$$

It is essentially a product of the absolute square of the reduced transition matrix $\bar{T}_{\boldsymbol{K}_i}$ and the p-α two-body differential cross section $d\sigma_{p\alpha}/d\Omega_{p\alpha}$ at a given scattering angle (energy) $\theta_{p\alpha}$ ($T_{p\alpha}$). To relate an off-the-energy-shell p-α scattering in the $(p, p\alpha)$ three-body kinematics to an on-shell observable, the final-state prescription of the on-shell approximation is adopted; $T_{p\alpha}$ is determined by the p-α relative momentum in the final state. The kinematical factor (or also referred to as the phase space factor) F_{kin} and a constant C_0 are defined by

$$F_{\mathrm{kin}} \equiv J_{\mathrm{L}} \frac{K_1 K_\alpha E_1 E_\alpha}{(\hbar c)^4} \left[1 + \frac{E_\alpha}{E_{\mathrm{B}}} + \frac{E_\alpha}{E_{\mathrm{B}}} \frac{\boldsymbol{K}_1 \cdot \boldsymbol{K}_\alpha}{K_\alpha^2}\right], \quad (4)$$

$$C_0 \equiv \frac{E_0}{(\hbar c)^2 K_0} \frac{\hbar^4}{(2\pi)^3 \mu_{p\alpha}^2}, \quad (5)$$

where $\mu_{p\alpha}$ is the reduced mass of the p-α binary system and J_{L} is the Jacobian from the center-of-mass frame to the L frame. The reduced transition matrix is given by

$$\bar{T}_{\boldsymbol{K}_i} \equiv \int d\boldsymbol{R}\, F_{\boldsymbol{K}_i}(\boldsymbol{R}) y(R) Y_{00}(\hat{\boldsymbol{R}}), \quad (6)$$

$$F_{\boldsymbol{K}_i}(\boldsymbol{R}) \equiv \chi^{*(-)}_{1,\boldsymbol{K}_1}(\boldsymbol{R})\, \chi^{*(-)}_{\alpha,\boldsymbol{K}_\alpha}(\boldsymbol{R})\, \chi^{(+)}_{0,\boldsymbol{K}_0}(\boldsymbol{R})\, e^{-i\boldsymbol{K}_0 \cdot \boldsymbol{R} A_\alpha / A}, \quad (7)$$

where $A_\alpha = 4$, $A = 20$, and $\chi_{i,\boldsymbol{K}_i}$ is a distorted wave between particle i and A when $i = 0$, otherwise between i and B. The outgoing and incoming boundary conditions of the scattering waves are specified by the superscripts $(+)$ and $(-)$, respectively. Note that the S_α does not appear explicitly in

Eqs. (3)–(7) because it is already taken into account in the RWA.

III. RESULTS AND DISCUSSION

A. Numerical inputs

The RWA is calculated by AMD and the Laplace expansion method [12]. The Hamiltonian used in the AMD calculation is given by

$$\hat{H} = \sum_i \hat{t}_i - \hat{t}_{\text{c.m.}} + \sum_{i<j} \hat{v}_{NN} + \sum_{i<j} \hat{v}_{\text{Coul}}, \tag{8}$$

where $\hat{t}_i$, $\hat{t}_{\text{c.m.}}$, $\hat{v}_{NN}$, and $\hat{v}_{\text{Coul}}$ being the nucleon and the center-of-mass kinetic energies, effective nucleon-nucleon interaction, and the Coulomb interaction, respectively. As for $\hat{v}_{NN}$, the Gogny D1S interaction [31] is adopted. The obtained RWA [12] (AMD-RWA) is shown in Fig. 1, and its α spectroscopic factor is $S_\alpha = 0.26$.

The kinematical condition of the ^{20}Ne$(p, p\alpha)^{16}$O reaction is shown in Fig. 2. In the experiment [15] the so-called energy sharing distribution was measured; the emitted angle of p (α) is fixed at -70° (46.3°), and the proton emission energy T_p is varied in the range of 40–75 MeV. By the energy conservation, T_α is ranging from 55 to 21 MeV accordingly. The incident energy is set to 101.5 MeV and all the scattering particles are kept in the same plane. With such a kinematical setup with no recoil, i.e., the reaction residue being at rest in the final state, is achieved at around $T_p = 67$ MeV ($T_\alpha = 30$ MeV). The TDX has a peak at this condition reflecting the fact that the struck α is bound by an s orbit. For the optical potential of the incident and emitted protons, the EDAD1 optical potential of the Dirac phenomenology [32,33] is adopted. The highly reliable optical model parametrization by Michel *et al.* [34] is adopted for the α-^{16}O scattering in the final state. As shown in Fig. 1 of Ref. [34], this parametrization of the α-^{16}O optical potential provides excellent agreement with the α-^{16}O elastic scattering data up to very backward angles, ranging 30–150 MeV α incident energies.

Since θ_p and θ_α are fixed in the present $(p, p\alpha)$ kinematics, the required p-α differential cross section lies in the very limited range of $\theta_{p\alpha} = 84^\circ$–$86^\circ$ in the p-α center-of-mass frame and $E_{p\alpha} = 75$–100 MeV in the p-α laboratory frame. Its energy and angular dependence are obtained by the microscopic single-folding model [35] with a phenomenological α density and the Melbourne nucleon-nucleon g-matrix interaction [36]. As shown in the dashed line in Fig. 3, the calculated p-α differential cross section at 85 MeV deviates from the experimental data [37] by about a factor of 2 at around $\theta_{p\alpha} = 84^\circ$–$86^\circ$. In the following analysis the cross section is tuned by a factor of 2.0 (dotted line) to correctly reproduce the p-α cross section data. It should be noted that this correction is valid thanks to the limited range of required $\theta_{p\alpha}$, which is the outcome of the kinematical condition in which θ_p and θ_α are fixed in the ^{20}Ne$(p, p\alpha)^{16}$O experiment.

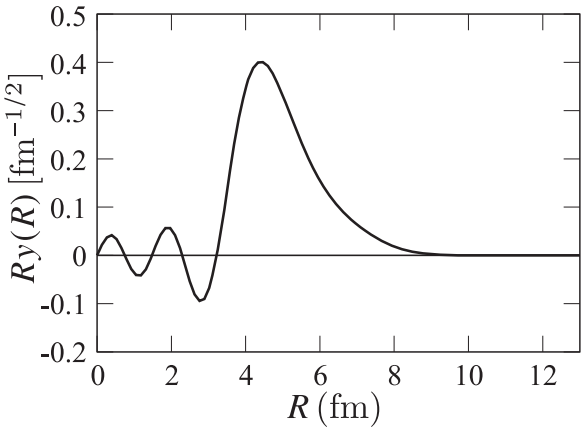

FIG. 1. $\alpha + {}^{16}$O RWA of the 0^+_1 state taken from Fig. 2 of Ref. [12].

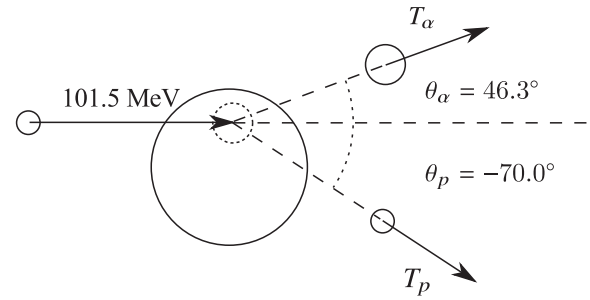

FIG. 2. Kinematical condition of the ^{20}Ne$(p, p\alpha)^{16}$O reaction [15].

B. α cluster wave function and ^{20}Ne$(p, p\alpha)^{16}$O cross section

In Fig. 4 the energy sharing distribution calculated by DWIA with the AMD-RWA is shown. The present framework well reproduces both the height and distribution of the experimental data [15] without any additional adjustment. Thus, the original problem, the inconsistency between the reaction analysis and the nuclear structure calculations, is resolved in the present approach. It should be stressed that the quantitative reproduction of the cross section data is guaranteed by the sophisticated RWA in ^{20}Ne, by the proper p-α cross section,

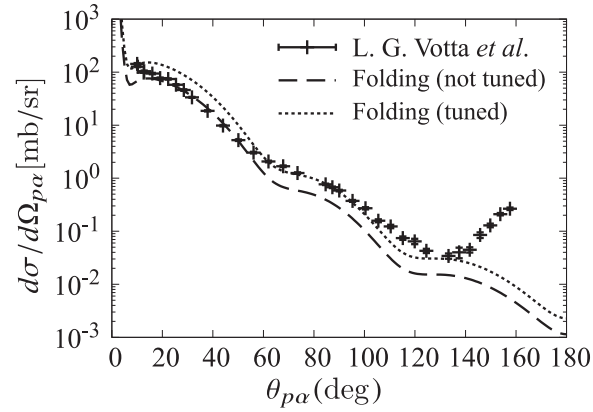

FIG. 3. p-α differential cross section at 85 MeV obtained by the folding model [35] with the Melbourne g-matrix interaction [36] (dashed line). The tuned result at around $\theta_{p\alpha} = 85^\circ$ is shown in dotted line. The experimental data are taken from Ref. [37].

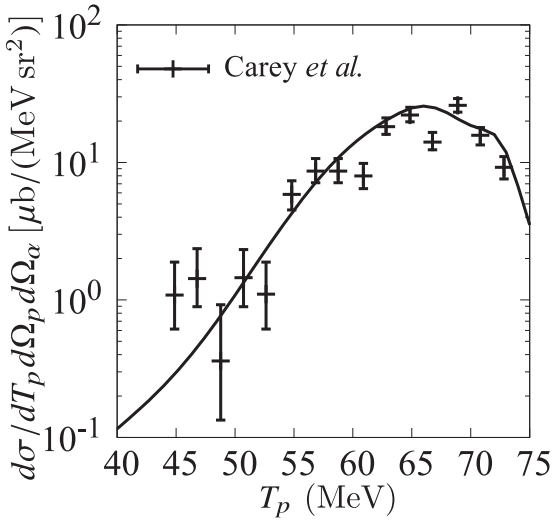

FIG. 4. The comparison between the calculated energy sharing distribution with the AMD-RWA (solid line) and the experimental data taken from Ref. [15].

and by the use of an appropriate α-^{16}O optical potential. In particular, α-^{16}O optical potential suggested in Ref. [34] was essential for this success of quantitative description. This result indicates that once the proper ingredients mentioned above are adopted, the $(p, p\alpha)$ reaction can be a quantitative probe for the α amplitude in the ground state of target nuclei.

Next, we investigate the relationship between the α cluster wave function and the α knockout cross section. Three different types of cluster wave functions shown in Fig. 5 are considered as artificial input data. They are constructed by superposing two Brink-Bloch (BB) wave functions [26] of the α-^{16}O cluster. The intercluster distances of the two BB wave functions are fixed at 3.0 fm and 5.5 fm, whereas the amplitude, C_1 and C_2, of these are varied by hand. In Table I, we show C_i $(i = 1$ or $2)$ and the resulting S_α of the three RWAs. As shown in Fig. 5, C_i of one labeled "original" (dashed) is determined so as to reproduce the largest peak and the tail behavior of the AMD-RWA as much as possible, while

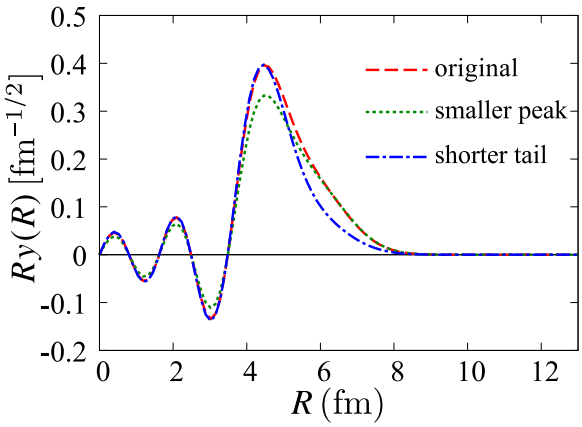

FIG. 5. RWAs constructed by the superposition of two Brink-Bloch wave functions of the α-^{16}O cluster. See text for details.

TABLE I. Coefficients for the BB wave functions. The resulting S_α are also shown.

	Original	Smaller peak	Shorter tail
C_1	0.67	0.55	0.69
C_2	0.17	0.17	0.09
S_α	0.24	0.18	0.21

for "smaller peak" (dotted) and "shorter tail" (dot-dashed), they are tuned to reduce the peak and tail region of the original RWA, respectively.

To investigate how these RWAs contribute to the TDX at the peak of the energy sharing distribution, it is useful to consider the transition matrix density (TMD) defined by [25]

$$\delta^{\rm Tr}(R) \equiv \bar{T}^*_{\boldsymbol{K}_i} \int d\Omega\, R^2 F_{\boldsymbol{K}_i}(\boldsymbol{R}) y(R) Y_{00}(\hat{\boldsymbol{R}}). \tag{9}$$

From Eq. (6) it has the following properties:

$$\int dR\, {\rm Re}[\delta^{\rm Tr}(R)] = \left|\bar{T}_{\boldsymbol{K}_i}\right|^2, \tag{10}$$

$$\int dR\, {\rm Im}[\delta^{\rm Tr}(R)] = 0. \tag{11}$$

Thus, one may regard ${\rm Re}[\delta^{\rm Tr}(R)]$ as a "radial distribution of the cross section" and its integrated value is proportional to the TDX. In Fig. 6 ${\rm Re}[\delta^{\rm Tr}(R)]$ at the recoilless condition ($T_p =$ 67 MeV) is shown. It is clearly seen that the internal region of the RWAs are suppressed by the absorption effect and the surface region contributes to the $(p, p\alpha)$ cross section. In Fig. 7 the energy sharing distributions with the RWAs of Fig. 5 are shown. The peak height of the energy sharing distribution is reduced significantly in the shorter tail case (dot-dashed), while it is similar to the original one in the smaller peak case (dotted), because of the peripherality of the reaction. Another response of the difference in the RWAs is the width of the energy sharing distribution. Since the RWA with smaller peak

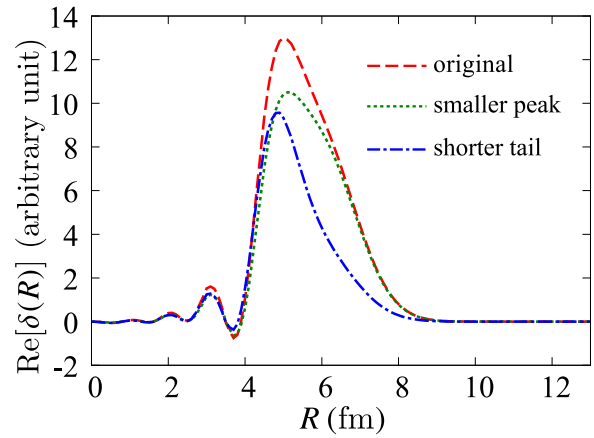

FIG. 6. Real part of the TMD at the recoilless condition: $T_p =$ 67 MeV. The dashed, dotted, and dot-dashed lines are the results with the RWAs shown by dashed, dotted, and dot-dashed lines in Fig. 5, respectively.

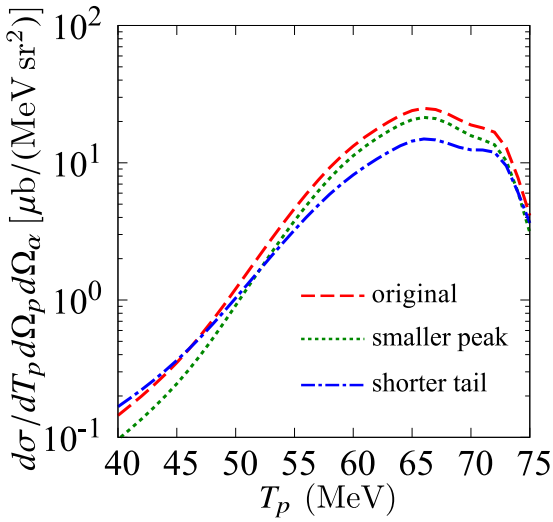

FIG. 7. Energy sharing distributions with the RWAs shown in Fig. 5.

(shorter tail) has narrower (wider) momentum distribution, its energy sharing distribution has a narrower (wider) width accordingly. From these results it is shown that the $(p, p\alpha)$ reaction is a quantitative probe for the α cluster state, putting emphasis on the α amplitude around the nuclear surface.

IV. SUMMARY

The ^{20}Ne$(p, p\alpha)^{16}$O reaction at 101.5 MeV was investigated within the DWIA framework. AMD was adopted to describe the α-^{16}O cluster state of ^{20}Ne and its RWA was obtained by the Laplace expansion method. It was found that by using reliable p-α differential cross section, distorting potentials as well as the AMD-RWA, the present DWIA calculation quantitatively reproduces the experimental data without any additional correction or scaling in describing the $(p, p\alpha)$ cross section. Thus, the inconsistency between the ^{20}Ne$(p, p\alpha)^{16}$O reaction analysis and the nuclear structure calculations is clearly resolved in the present approach.

By the analyses using the BB wave functions with different spatial distributions and corresponding α spectroscopic factors, it was shown that the surface region of the target is selectively probed by the ^{20}Ne$(p, p\alpha)^{16}$O reaction. Therefore the $(p, p\alpha)$ reaction is a good probe for the surface amplitude of the cluster wave function, which should be directly related to the α clustering of interest. One may also deduce the momentum distribution of the α cluster wave function from the width of the energy sharing distribution. For the momentum distribution of the α cluster to be extracted, the $(p, p\alpha)$ cross section should be measured very precisely down to the tail region.

ACKNOWLEDGMENTS

This work was supported in part by Grants-in-Aid of the Japan Society for the Promotion of Science (Grants No. JP18K03617, No. JP16K05352, No. JP19K03859, and No. JP16K05339), the Hattori Hokokai Foundation Grant-in-Aid for Technological and Engineering Research, and by the grant for the RCNP joint research project.

[1] K. Ikeda, N. Takigawa, and H. Horiuchi, Prog. Theor. Phys. Suppl. **E68**, 464 (1968).
[2] M. Freer, H. Horiuchi, Y. Kanada-En'yo, D. Lee, and Ulf-G. Meißner, Rev. Mod. Phys. **90**, 035004 (2018).
[3] Y. Kanada-En'yo, H. Horiuchi, and A. Ono, Phys. Rev. C **52**, 628 (1995).
[4] Y. Kanada-En'yo, Phys. Rev. Lett. **81**, 5291 (1998).
[5] Y. Kanada-En'yo and H. Horiuchi, Prog. Theor. Phys. Suppl. **142**, 205 (2001).
[6] M. Kimura, Phys. Rev. C **69**, 044319 (2004).
[7] Y. Kanada-En'yo, M. Kimura, and A. Ono, Prog. Theor. Exp. Phys. **2012**, 01A202 (2012).
[8] M. Kimura, T. Suhara, and Y. Kanada-En'yo, Eur. Phys. J. A **52**, 373 (2016).
[9] Y. Chiba, M. Kimura, and Y. Taniguchi, Phys. Rev. C **93**, 034319 (2016).
[10] Y. Kanada-En'yo, Phys. Rev. C **93**, 024322 (2016).
[11] Y. Kanada-En'yo, Phys. Rev. C **93**, 054307 (2016).
[12] Y. Chiba and M. Kimura, Prog. Theor. Exp. Phys. **2017**, 053D01 (2017).
[13] P. G. Roos, N. S. Chant, A. A. Cowley, D. A. Goldberg, H. D. Holmgren, and R. Woody, III, Phys. Rev. C **15**, 69 (1977).
[14] A. Nadasen, N. S. Chant, P. G. Roos, T. A. Carey, R. Cowen, C. Samanta, and J. Wesick, Phys. Rev. C **22**, 1394 (1980).
[15] T. A. Carey, P. G. Roos, N. S. Chant, A. Nadasen, and H. L. Chen, Phys. Rev. C **29**, 1273 (1984).
[16] C. W. Wang, P. G. Roos, N. S. Chant, G. Ciangaru, F. Khazaie, D. J. Mack, A. Nadasen, S. J. Mills, R. E. Warner, E. Norbeck, F. D. Becchetti, J. W. Janecke, and P. M. Lister, Phys. Rev. C **31**, 1662 (1985).
[17] A. Nadasen, P. G. Roos, N. S. Chant, C. C. Chang, G. Ciangaru, H. F. Breuer, J. Wesick, and E. Norbeck, Phys. Rev. C **40**, 1130 (1989).
[18] T. Yoshimura, A. Okihana, R. Warner, N. Chant, P. Roos, C. Samanta, S. Kakigi, N. Koori, M. Fujiwara, N. Matsuoka, K. Tamura, E. Kubo, and K. Ushiro, Nucl. Phys. A **641**, 3 (1998).
[19] R. Neveling, A. A. Cowley, Z. Buthelezi, S. V. Förtsch, H. Fujita, G. C. Hillhouse, J. J. Lawrie, G. F. Steyn, F. D. Smit, S. M. Wyngaardt, N. T. Botha, L. Mudau, and S. S. Ntshangase, Phys. Rev. C **77**, 037601 (2008).
[20] J. Mabiala, A. A. Cowley, S. V. Förtsch, E. Z. Buthelezi, R. Neveling, F. D. Smit, G. F. Steyn, and J. J. Van Zyl, Phys. Rev. C **79**, 054612 (2009).
[21] K. Yoshida, K. Minomo, and K. Ogata, Phys. Rev. C **94**, 044604 (2016).
[22] M. Lyu, K. Yoshida, Y. Kanada-En'yo, and K. Ogata, Phys. Rev. C **97**, 044612 (2018).
[23] K. Yoshida, K. Ogata, and Y. Kanada-En'yo, Phys. Rev. C **98**, 024614 (2018).
[24] N. S. Chant and P. G. Roos, Phys. Rev. C **27**, 1060 (1983).
[25] T. Wakasa, K. Ogata, and T. Noro, Prog. Part. Nucl. Phys. **96**, 32 (2017).

[26] D. M. Brink, in *Proceedings of the International School of Physics "Enrico Fermi", Course 36, Varenna*, edited by C. Bloch (Academic Press, New York, 1966), p. 247.
[27] F. Nemoto and H. Bandō, Prog. Theor. Phys. **47**, 1210 (1972).
[28] T. Matsuse, M. Kamimura, and Y. Fukushima, Prog. Theor. Phys. **53**, 706 (1975).
[29] Y. Fujiwara, Prog. Theor. Phys. **62**, 122 (1979).
[30] Y. Kanada-En'yo, T. Suhara, and Y. Taniguchi, Prog. Theor. Exp. Phys. **2014**, 073D02 (2014).
[31] J. Berger, M. Girod, and D. Gogny, Comput. Phys. Commun. **63**, 365 (1991).
[32] S. Hama, B. C. Clark, E. D. Cooper, H. S. Sherif, and R. L. Mercer, Phys. Rev. C **41**, 2737 (1990).
[33] E. D. Cooper, S. Hama, B. C. Clark, and R. L. Mercer, Phys. Rev. C **47**, 297 (1993).
[34] F. Michel, J. Albinski, P. Belery, T. Delbar, G. Grégoire, B. Tasiaux, and G. Reidemeister, Phys. Rev. C **28**, 1904 (1983).
[35] M. Toyokawa, K. Minomo, and M. Yahiro, Phys. Rev. C **88**, 054602 (2013).
[36] K. Amos, P. J. Dortmans, H. V. von Geramb, S. Karataglidis, and J. Raynal, Adv. Nucl. Phys. **25**, 276 (2000).
[37] L. G. Votta, P. G. Roos, N. S. Chant, and R. Woody, Phys. Rev. C **10**, 520 (1974).